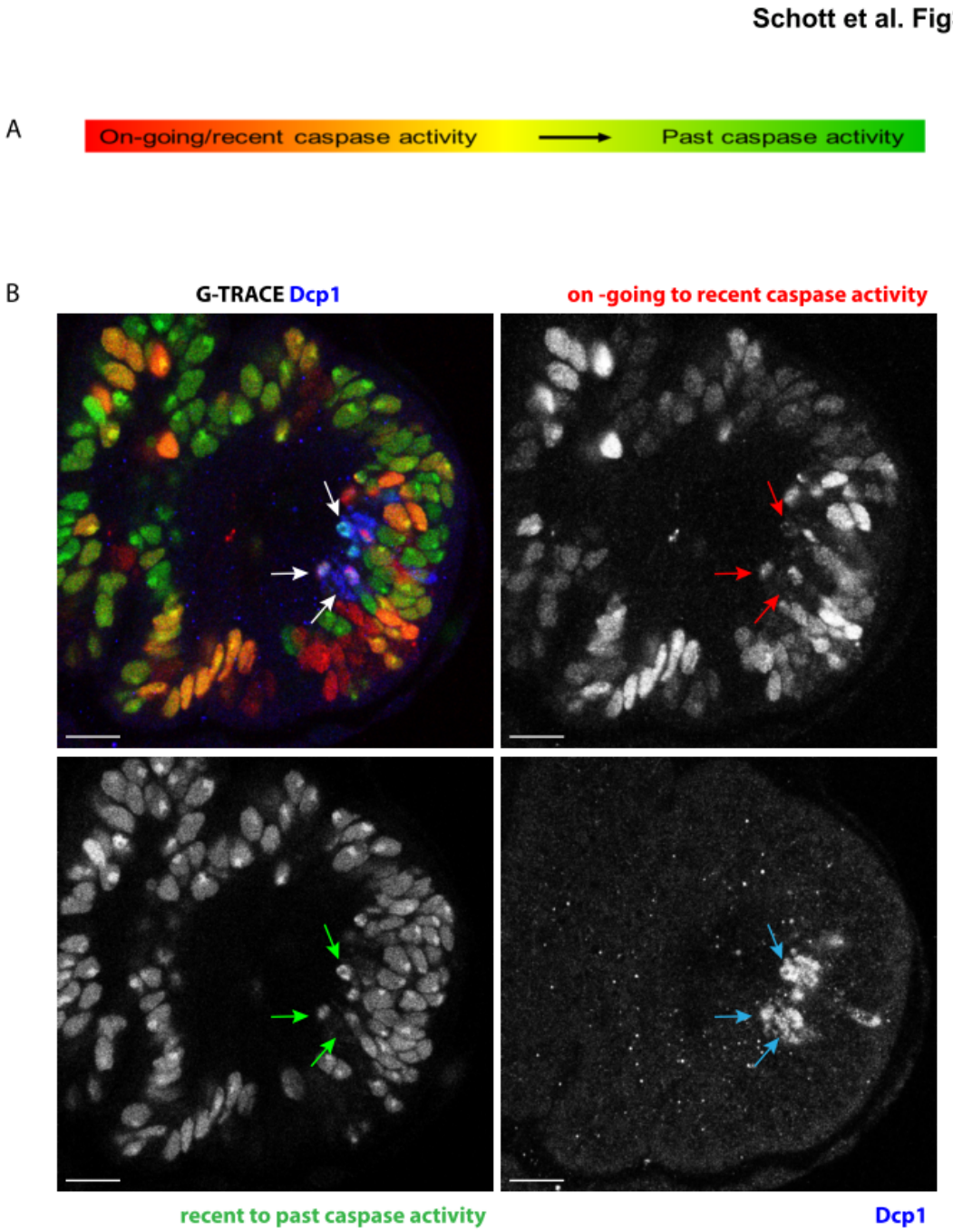

Figure S1: Activity of the caspase sensitive Gal4 sensor in the leg. A) Frieze representing the time scale labelling of caspase activity according to (Tang et al., 2015). (B) Pupal leg disc showing a wide expression of both nuclear GFP and RFP under the control of the caspase sensitive Gal4 sensor, while very few cells are positive for Dcp1 (arrows), suggesting that this caspase sensitive Gal4 can detect very low level of caspase activity, not always associated with death. Scale bar10µm, N=10.

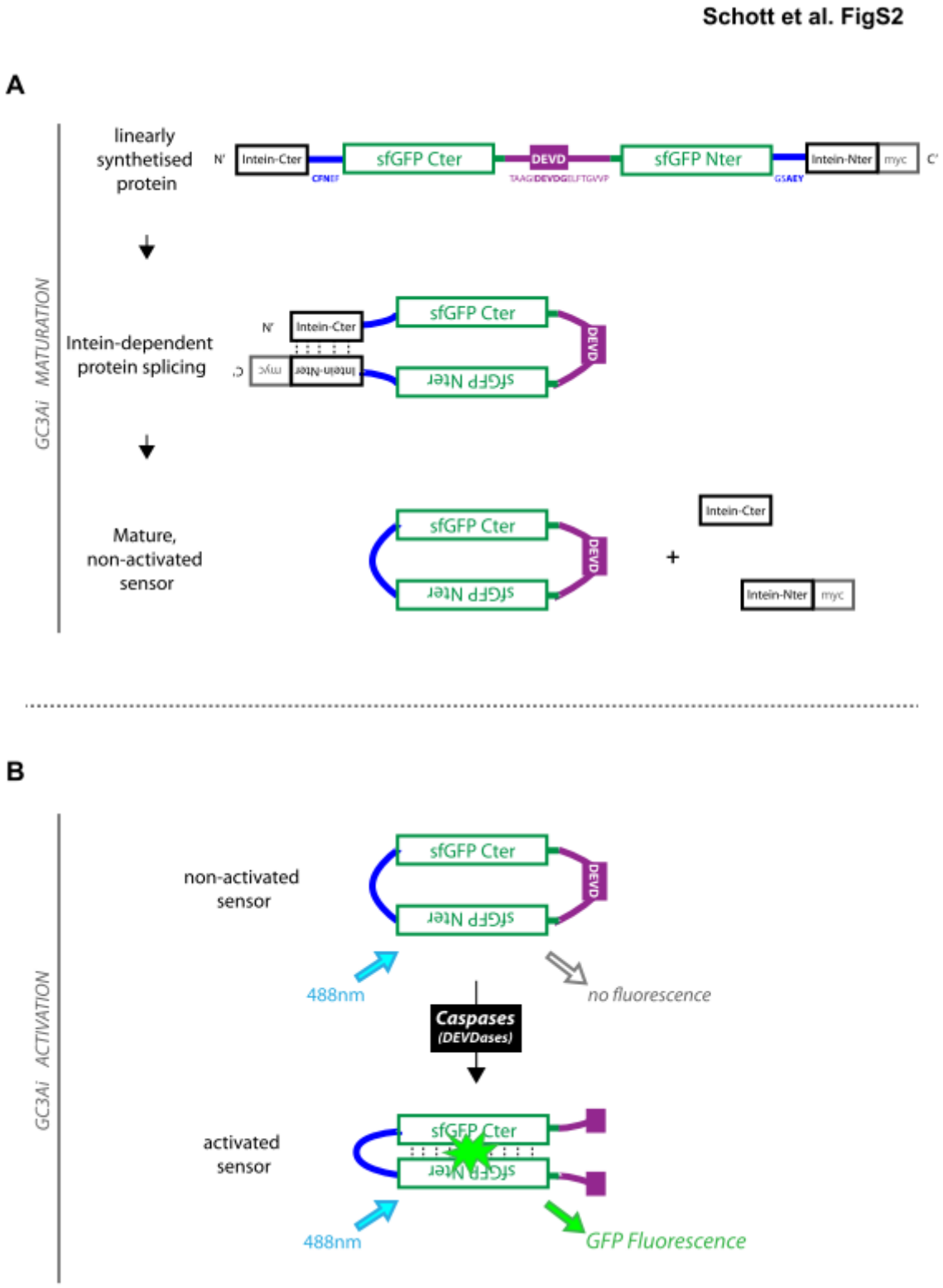

Figure S2. GC3Ai apoptosensor maturation and activation modes. Detailed scheme of the GFP sensor Caspase-3-like protease Activity Indicator (GC3Ai): the C and N termini of the GFP have been linked by a fragment containing a DEVD caspase cleavage site in such a way that DEVD needs to be cleaved in order for the GFP to fluoresce; while intein domains have been added at the new N' and C'

termini of the molecule, allowing the molecule to be circularized after intein dependent protein splicing (see (Zhang et al., 2013).

Schott et al. FigS3

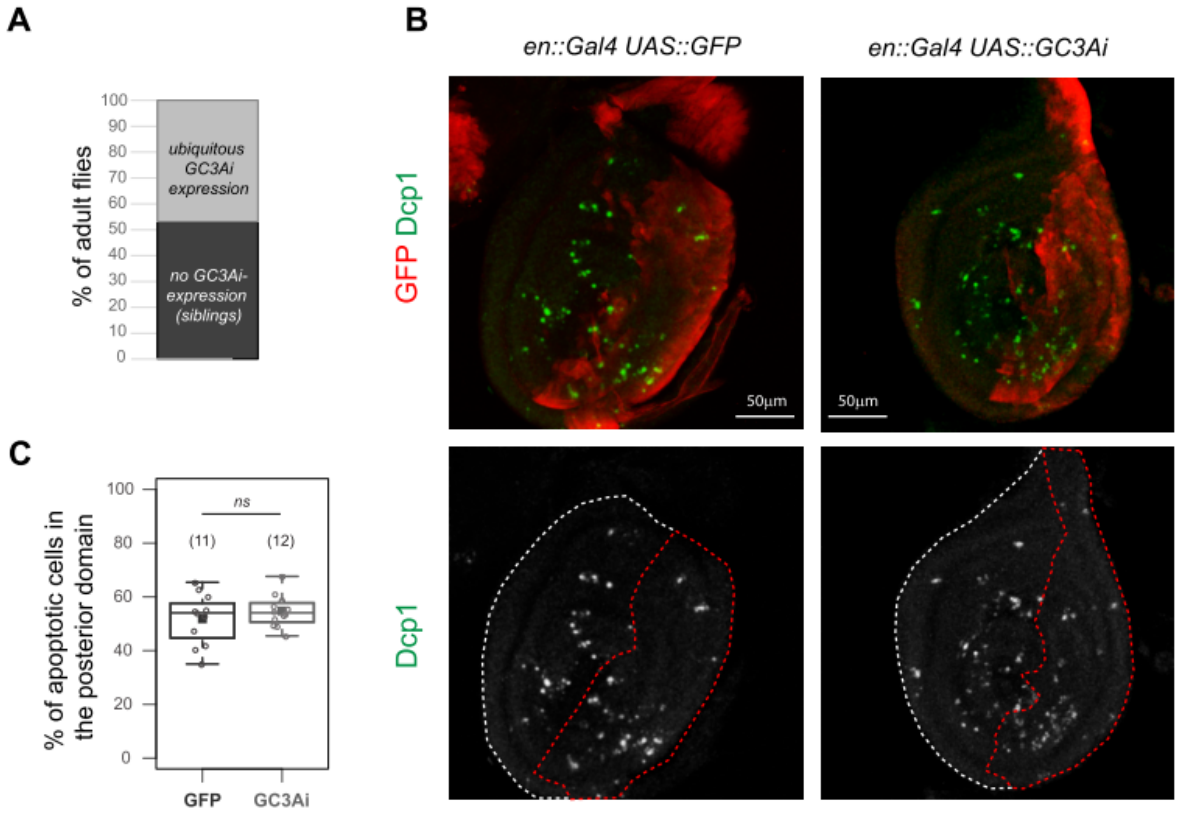

Figure S3. Effects of GC3Ai expression on viability and apoptotic pattern. (A) Comparison of the number of adult flies issued from the same cross between *act::Gal4 / CyO* and *uas::GC3Ai / uas::GC3Ai* flies (n=256 individuals in total). (B) Apoptotic pattern visualized by an anti-activated Dcp1 staining (green or white) in *en::Gal4>uas::GFP* (control) and *en::Gal4>uas::GC3Ai* leg discs. (C) Quantifications of apoptotic cells in the posterior domain (see M&M, n=11 and 12 respectively).

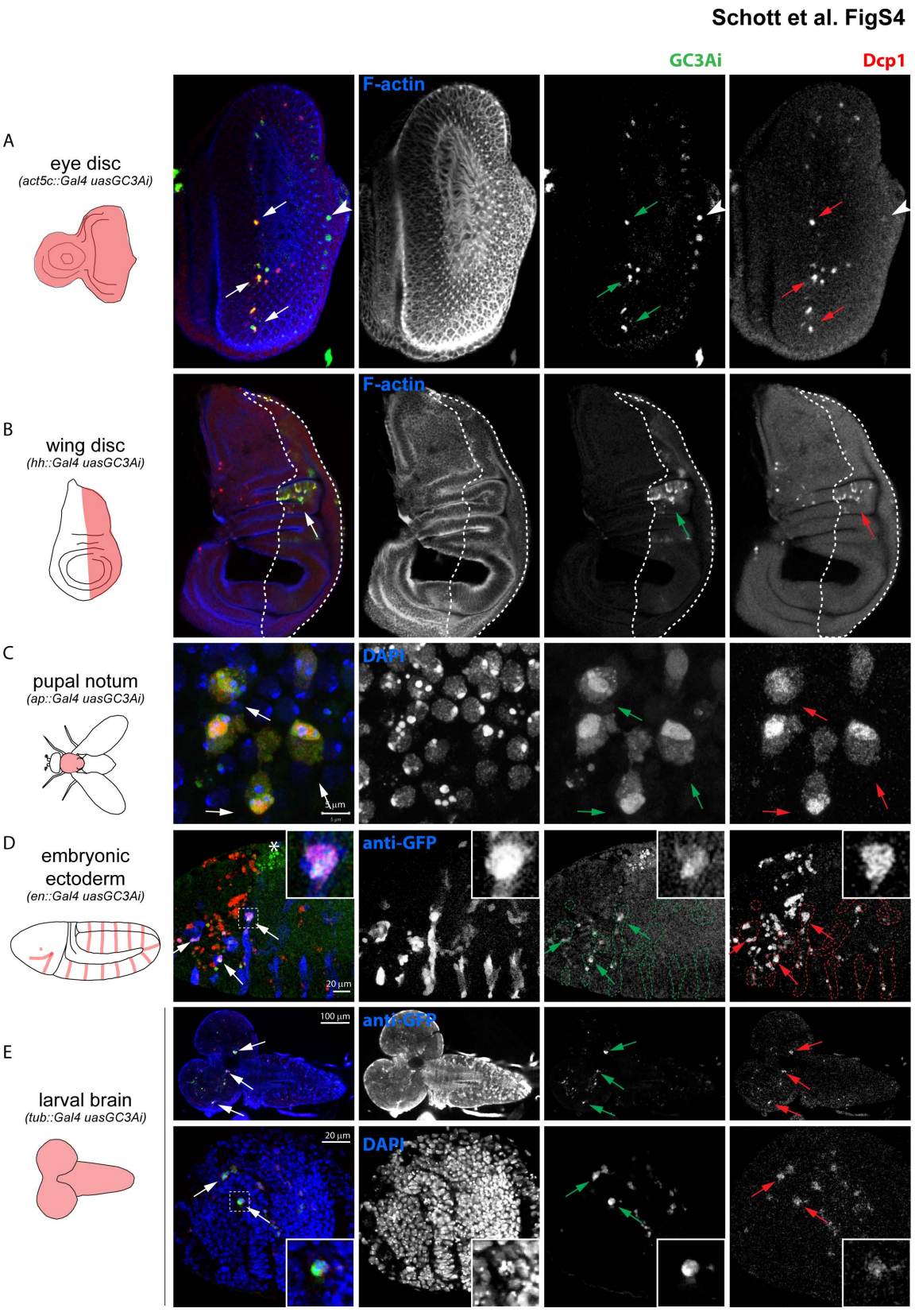

Figure S4. Pattern of GC3Ai fluorescence in various *Drosophila* tissues. (A-E) On the left are presented schemes of the different tissues showing the domain in which GC3Ai has been expressed. On the right, the GC3Ai activation pattern and activated Dcp1 antibody staining is shown. (A) Fixed eye discs (n=6) from *act::Gal4>uas::GC3Ai* L3 larvae. Note the presence of some GC3Ai positive

cells in which Dcp1 is not detectable yet, that could correspond to early apoptotic cells as shown in Fig3 (arrowhead). (B) Fixed wing imaginal discs from *hh::Gal4>uas::GC3Ai* L3 larvae (n=6). (C) Pupal notum from *ap::Gal4>uas::GC3Ai* (n=60 cells). (D) Ectoderm from *en::Gal4>uas::GC3Ai* embryos (n=8). (E) Larval central nervous system from *tub::Gal4>uas::GC3Ai* (n=7). Note the co-detection of GC3Ai and Dcp1 activation in each of these tissues (arrows).

Schott et al. FigS5

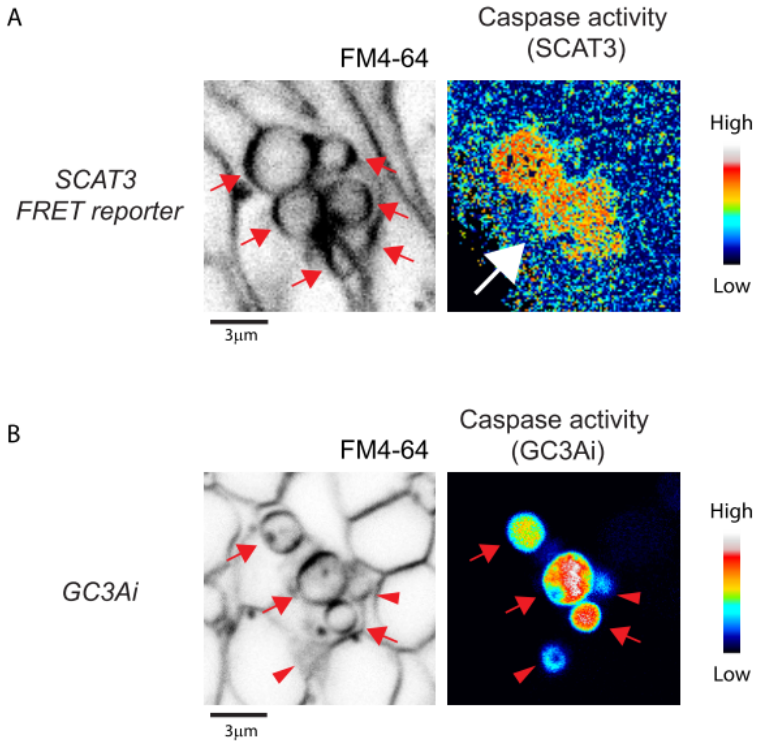

Figure S5: Caspase activity detection by SCAT3 FRET reporter and GC3Ai. A-B. Images of living tissues showing SCAT3 FRET reporter activity (A) or GC3Ai activity (B) using a color-code to report FRET ratio or fluorescence intensity. The highest intensity of caspase activity is in white while the lowest intensity is in black (see intensity scale). Labelling of the plasma membrane (black) is achieved using the lipid-binding vital dye FM4-64 which allows to detect apoptotic bodies. (A) On the left, six apoptotic bodies are detected (red arrows). On the right, the caspase activity detected by the FRET reporter highlights the dying cell (big white arrow), but individual apoptotic bodies are not clearly visible (n=15/24). (B) On the left, 3 apoptotic bodies are detected (red arrows) and on the right

GC3Ai detects all of them (red arrows) (n= 20/21). Two apoptotic bodies are slightly out of focus and indicated with arrowheads.

Schott et al. FigS6

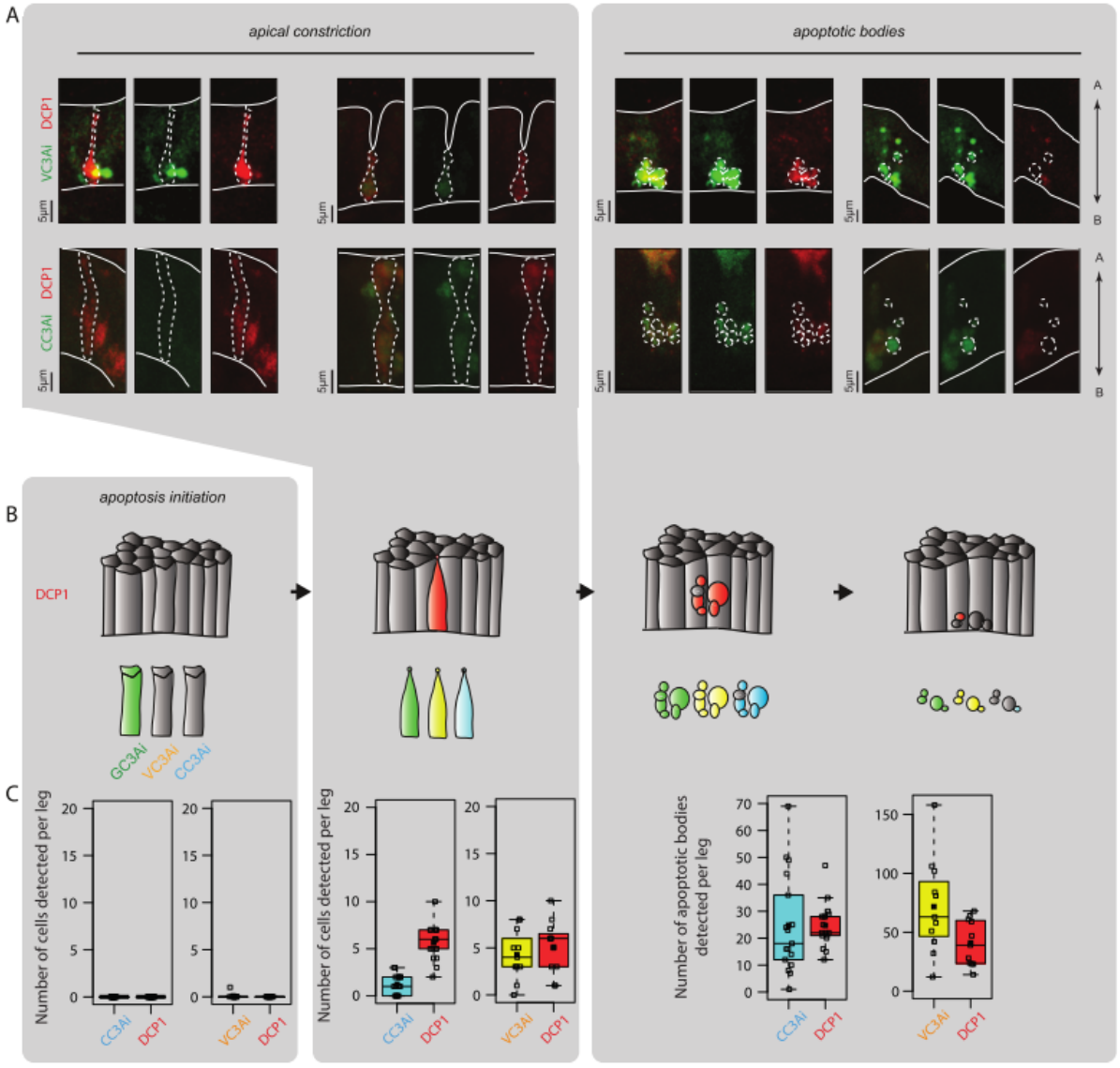

Figure S6. Pattern of fluorescence of Venus (VC3Ai) and Cerulean (CC3Ai) apoptosensors. (A-C) VC3Ai, CC3Ai and Dcp1 activation patterns are compared in pupal leg discs. Successive stages of the apoptotic process are presented from left to right. (A) Confocal images showing the comparison between VC3Ai (green), CC3Ai (green) and Dcp1 (red) activation patterns in fixed pupal leg discs at different apoptotic stages. Apoptotic cells or apoptotic bodies are surrounded by white dotted lines and the apical and basal surfaces of the epithelium are represented by a white line. (B) Schemes of the

different apoptotic stages recapitulating the activation pattern of VC3Ai (yellow) or CC3Ai (cyan) in fixed tissues, compared to Dcp1 (red). The pattern of GC3Ai fluorescence, as determined on fixed tissues in figure 3, is shown in green for comparison. (C) Quantification of the number of VC3Ai (yellow), CC3Ai (cyan) and Dcp1 (red) positive apoptotic cells or apoptotic bodies counted per fixed leg disc according to the different apoptotic stages (n=11 legs for VC3Ai, n=17 legs for CC3Ai). Data are presented as box plots showing every leg disc (open squares) as well as the mean (filled square).

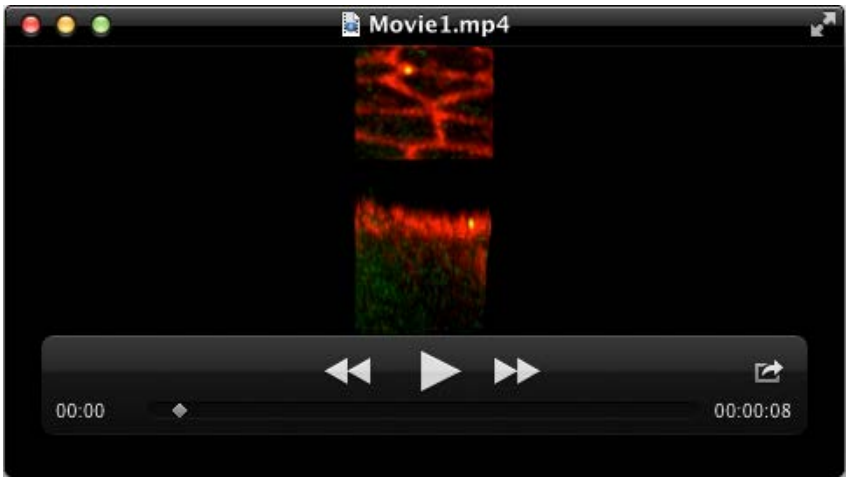

Movie 1. Time lapse of a subset of a pupal leg disc expressing alphaCat-TagRFP in the ap domain (which encompasses the t4-t5 fold) and the GC3Ai construct to reveal caspase activity and thus visualise apoptotic cell. The apoptotic cell shape can be followed on the apical (top) and sagittal (bottom) sections. Note the reduction of the apical surface of the apoptotic cell on the apical views, the transient deformation of the apical surface on the sagittal views and the formation of apoptotic bodies.